Journal of Mathematical Modeling
Vol. -, No. -, 2026, pp. -. Research Article

JMM

Mittag-Leffler wavelet-based numerical method for fractional pantograph delay differential equations

Arezoo Ghasempour[†], **Yadollah Ordokhani**[†*], **Mohsen Razzaghi**[‡]

[†]*Department of Mathematics, Faculty of Mathematical sciences, Alzahra University, Tehran, Iran*
[‡]*Department of Mathematics and Statistics, Mississippi State University, MS, USA*
Email(s): a.ghasempour@alzahra.ac.ir, ordokhani@alzahra.ac.ir, razzaghi@math.msstate.edu

Abstract. This paper proposes a robust numerical framework for solving fractional pantograph delay differential equations and time-fractional partial pantograph delay differential equations. The approach leverages the Riemann–Liouville fractional integral operator, represented through Mittag-Leffler wavelet functions within a collocation-based scheme. To facilitate computation, an operational matrix is constructed, enabling the transformation of the fractional differential system into a system of algebraic equations. The proposed method's accuracy, stability, and convergence are rigorously validated through comprehensive numerical experiments.

Keywords: Fractional pantograph differential equations, time-fractional partial pantograph delay differential equations, Mittag-Leffler wavelets, operational matrix
AMS Subject Classification 2010: 34A08, 26A33.

1 Introduction

Fractional calculus has its origins in the 16th century when L'Hopital questioned Leibniz in 1695 over a derivative of order $\frac{1}{2}$. Consequently, the past two decades have witnessed a marked rise in interest in fractional calculus across various scientific fields. The subject's early development and history are covered in [13].

Our work is devoted to numerical solutions for various categories of fractional partial differential equations. Delay differential equations (DDEs) play a critical role in numerous scientific and engineering applications. These equations model systems whose behavior depends on both their current and past states. This capability allows DDEs to accurately represent the inherent time delays observed in many real-world processes [29]. As a result, researchers have devoted significant attention to developing both analytical and numerical solution methods. Among the various types, pantograph DDEs (PDDEs) have

*Corresponding author
Received: 04 August 2025/ Revised: 02 October 2025/ Accepted: 23 November 2025
DOI: 10.22124/jmm.2025.31321.2807

attracted particular interest due to their complex structure and wide range of applications [12]. Fractional DDEs (FDDEs) serve as powerful tools for modeling systems exhibiting memory and hereditary properties. In particular, PDDEs play a key role in areas such as electrodynamics, control engineering, hydraulic networks, biological systems, and long transmission lines. These equations inherently account for history-dependent dynamics and delayed effects, which are not captured by conventional integer-order models. Although some initial problems may appear straightforward, the fractional characteristics of these equations ensure their practical significance, underscoring the need for robust numerical solution techniques [9].

Finding exact solutions for PDDEs is often challenging. Therefore, approximate and numerical techniques have become essential. Several methods have been proposed, such as the spectral method [16], the fractional-order Bernoulli wavelet method [22], the fractional-order Boubaker polynomial approach [21], the Taylor collocation method [27], the Legendre wavelets method [23], the generalized differential transform method [18], and the modified predictor-corrector scheme [17].

To solve PDDEs, iterative strategies based on reformulating them as integral equations have been applied [6]. The Vieta–Lucas series has been used to handle multi-PDDEs with singularities [11]. Additionally, the homotopy perturbation method has been employed to obtain both exact and approximate solutions [1]. More recently, Hajishafieiha et al. introduced a novel class of polynomials for numerically solving fractional nonlinear multi-PDDEs [8]. Senol et al. [26] studied the (2+1)-dimensional conformable combined potential Kadomtsev–Petviashvili-BKP equation, which appears in fluid dynamics, plasma physics, and nonlinear optics. They applied the Residual Power Series Method (RPSM) to obtain accurate approximate solutions and to validate analytical results. This modern approach provides a reliable tool for solving fractional differential equations and complements the wavelet-based method presented in the current study.

In this field, FDDEs, which have received relatively little attention in terms of numerical and analytical methods, present significant computational challenges that require novel approaches. Das et al. [5] introduced an operator-based iterative approach for nonlinear fractional Volterra integro-differential equations by first reducing them to a second-kind form. For solving multi-term time fractional partial integro-differential equations with Volterra integral operators that exhibit mild singularities at initial time, Santra et al. [24] introduced a higher-order approximation method on an adaptive graded mesh. For solving weakly singular Volterra integro-differential equations of fractional order, Das and Rana [3] developed an operator-based parameterized method with residual minimization. The authors proposed an efficient finite difference scheme to address singularly perturbed parabolic convection–diffusion problems involving a large time-lag [15].

Mittag–Leffler polynomials are important in numerical computation due to their exponential-like properties and Sheffer sequence structure. Their simple recurrence relations and explicit generating functions facilitate series expansions and function approximations. The limited number of terms produces sparse matrices, reducing computational cost and memory use, while closed-form coefficients improve numerical stability. Their natural connection to fractional operators makes them especially effective for solving fractional differential equations and modeling complex systems [7].

Wavelet-based methods have attracted attention for their spectral accuracy and flexibility in solving PDDEs. While classical polynomials like Bernoulli, Legendre, and Gegenbauer [10,22,28] are effective, they lack a natural connection to fractional calculus operators. The Mittag-Leffler function [19], naturally arises in fractional differential equations. Wavelets based on Mittag-Leffler polynomials provide a more efficient basis, capturing the non-local and singular behavior of fractional operators with higher accuracy

and faster convergence. This work develops a novel numerical scheme leveraging these advantages.

This work is concerned the following problems:

Problem 1. Fractional PDDEs:

$$D^{\gamma}u(x) = a_0(x)u(x) + \sum_{l=1}^{L} a_l(x)D^{\eta}u(\tau_l x) + \chi(x), \quad 0 \le x \le 1, \tag{1}$$

where $n-1 < \gamma \le n$, $n \in \mathrm{N}$, and $0 \le \eta_l \le \gamma$. Here the functions $\chi(x)$ and $a_l(x)$ for $l = 1,2,...,L$, are known functions, and the pantograph parameters are represented by the values $0 < \tau_l \le 1$. Furthermore, the problem is subject to the following initial conditions:

$$u^{(s)}(0) = p_s, \qquad s = 0,1,...,n-1,$$

where known constants p_s belong to R.

Problem 2. Time-fractional partial PDDEs:

$$\frac{\partial^{\gamma}}{\partial t^{\gamma}}u(x,t) = F\left(x,t,u(p_0x,q_0t), \frac{\partial u}{\partial x}(p_1x,q_1t), \frac{\partial^2 u}{\partial x^2}(p_2x,q_2t)\right), \tag{2}$$

for $x \in [0,1]$, $t \in [0,1]$, and $0 < \gamma \le 1$, where $p_i, q_i \in (0,1]$ are delay parameters for $i = 0,1,2$. The equation is subject to the initial condition:

$$u(x,0) = \phi(x), \quad x \in [0,1], \tag{3}$$

and the boundary conditions:

$$u(0,t) = \psi_0(t), \quad u(1,t) = \psi_1(t), \quad t \in [0,1]. \tag{4}$$

To address these equations efficiently, Riemann–Liouville fractional integral (RLFI) operator, Laplace transform, and Mittag–Leffler wavelet functions are employed. By expressing the solution in terms of these wavelets and applying the corresponding operators, the fractional PDDEs is converted into a system of algebraic equations, which can be solved effectively.

The structure of the paper is as follows: In Section 2, we present the essential notations and mathematical preliminaries, including Mittag-Leffler polynomials, wavelet functions, and the operational matrix associated with the RLFI. Section 3 outlines the construction of the proposed numerical scheme. A rigorous error analysis is carried out in Section 4 to establish the theoretical accuracy of the method. Section 5 is dedicated to numerical experiments that validate the performance and efficiency of the proposed approach through various illustrative examples. Concluding remarks are discussed in Section 6.

2 Notation

This section introduces the key definitions and notations that will be used throughout the article.

Definition 1. *The symbol $I^{\gamma}f(x)$ represents the RLFI operator applied to the function $f(x)$. For a function f which is locally integrable on $[0,\infty)$, i.e., $f \in L^1_{loc}[0,\infty)$, and is formally defined as follows [19]:*

$$\begin{aligned} I^{\gamma}f(x) &= \frac{1}{\Gamma(\gamma)}\int_0^x (x-s)^{\gamma-1}f(s)ds = \frac{1}{\Gamma(\gamma)}x^{\gamma-1} \star f(x), \quad x \ge 0, \quad \gamma > 0, \\ I^0 f(x) &= f(x), \end{aligned} \tag{5}$$

where $x^{\gamma-1} \star f(x)$ denotes the convolution product of $x^{\gamma-1}$ and $f(x)$. The RLFI satisfies the following properties:

$$I^{\gamma}x^{\beta} = \frac{\Gamma(\beta+1)}{\Gamma(\beta+\gamma+1)}x^{\gamma+\beta}, \quad \beta > -1. \tag{6}$$

Definition 2. *The Caputo fractional derivative of the function $f(x)$, denoted by $D^{\gamma}f$, is defined as follows for functions f such that $f^{(n-1)}$ is absolutely continuous on $[0,T]$ for any $T > 0$ (ensuring $f^{(n)} \in L^1_{loc}[0,\infty)$) [19]:*

$$D^{\gamma}f(x) = \frac{1}{\Gamma(n-\gamma)}\int_0^x \frac{f^n(s)ds}{(x-s)^{\gamma-n+1}}, \quad x > 0, 0 \leqslant n-1 < \gamma < n. \tag{7}$$

The Caputo fractional derivative possesses the following properties:

$$I^{\gamma}D^{\gamma}f(x) = f(x) - \sum_{i=0}^{n-1} f^{(i)}(0)\frac{x^i}{i!}, \tag{8}$$

$$D^{\gamma}x^{\beta} = \begin{cases} 0, & \gamma \in N_0, \quad \beta < \gamma, \\ \frac{\Gamma(\beta+1)}{\Gamma(\beta+1-\gamma)}x^{\beta-\gamma}, & otherwise. \end{cases} \tag{9}$$

We present a geometric interpretation of fractional operators to clarify their conceptual significance. The Riemann-Liouville integral $I^{\gamma}f(x)$, as defined in Eq. (5), can be viewed as the "area of a shadow." By writing it as a Stieltjes integral $\int_0^x f(s)dg_x(s)$ with a suitably scaled function $g_x(s)$, the integral corresponds to the projected area of the curve $(s, g_x(s), f(s))$ onto the (g,f)-plane, providing an intuitive visualization beyond the classical notion of area under a curve. Physically, if x represents individual time (e.g., a local clock) and $v(s)$ denotes velocity, then $I^{\gamma}v(x)$ represents the actual distance traveled within a non-uniform cosmic time $T = g_x(s)$, capturing dynamic effects such as gravitational field variations. Conversely, the Caputo derivative $D^{\gamma}S(x)$, defined in Eq. (7), acts as an inverse operator, recovering the local velocity $v(x)$ from the distance $S(x)$ measured in cosmic time.

This two-time framework naturally explains the presence of historical initial conditions in Caputo derivatives (see Eq. (8)), as the system's past evolution in cosmic time influences the state at the initial individual time $x = 0$ [20].

2.1 Mittag-Leffler polynomials

Originally introduced by Mittag-Leffler in 1891, the polynomials $ML_n(x)$ are defined as follows [7]:

$$ML_n(x) = \sum_{k=0}^{n} \left(\begin{array}{c} n \\ k \end{array} \right) (n-1)_{n-k}2^k(x)_k. \tag{10}$$

The notation $(x)_n$ represents the falling factorial, given by $(x)_n = x(x-1)\cdots(x-(n-1))$, where $n \geqslant 0$. One has

$$ML_n(x+s) = \sum_{k=0}^{n} \left(\begin{array}{c} n \\ k \end{array} \right) ML_k(x)ML_{n-k}(s). \tag{11}$$

In addition, these polynomials satisfy the following recurrence relation:

$$ML_{n+1}(x) = 2xML_n(x) + n(n-1)ML_{n-1}(x). \tag{12}$$

Proposition 1. *As stated in Vieta's formulas [7], the falling factorial* $(x)_n$ *is related as:*

$$(x)_n = x(x-1)\dots(x-(n-1)) = x^n - (\sum_{j=0}^{n-1} j)x^{(n-1)} + (\sum_{0\le j<i\le n-1} ji)x^{(n-2)} + \dots + (-1)^n(\prod_{j=0}^{n-1} j) = \sum_{k=0}^{n-1} A_k x^k. \tag{13}$$

2.2 Wavelet functions

The formula below defines a family of wavelet functions known as the Mittag-Leffler wavelets on the interval $[0,1)$. By applying Eq. (10), we obtain

$$\vartheta_{n,m}(x) = \begin{cases} 2^{\frac{k-1}{2}}\mathscr{M}_m\left(2^{k-1}x-n+1\right), & x\in\left[\frac{n-1}{2^{k-1}},\frac{n}{2^{k-1}}\right), \\ 0, & \text{otherwise}, \end{cases} \tag{14}$$

where

$$\mathscr{M}_m\left(2^{k-1}x-n+1\right) = \frac{1}{\sqrt{\int_0^1 ML_m^2(x)dx}} \times ML_m(2^{k-1}x-n+1). \tag{15}$$

In this context, $n = 1,2,\dots,2^{k-1}$, with k being an arbitrary positive integer, $m = 0,1,\dots,M-1$ indicates the degree of the Mittag-Leffler polynomials, and x corresponds to the normalized time variable.

2.3 Riemann-Liouville operational matrix

This part calculates the Riemann-Liouville operational matrix of Mittag-Leffler wavelets. We now derive the operator I^γ for $\vartheta(x)$ as defined:

$$I^\gamma\vartheta(x) = \tilde{\vartheta}(x,\gamma), \tag{16}$$

where

$$\vartheta(x) = \left[\vartheta_{1,0}(x),\dots,\vartheta_{1,M-1}(x),\ \vartheta_{2,0}(x),\dots,\vartheta_{2,M-1}(x),\ \dots,\ \vartheta_{2^{k-1},0}(x),\dots,\vartheta_{2^{k-1},M-1}(x)\right]^T, \tag{17}$$

and

$$\tilde{\vartheta}(x,\gamma) = \left[I^\gamma\vartheta_{1,0}(x),\dots,I^\gamma\vartheta_{1,M-1}(x),\ I^\gamma\vartheta_{2,0}(x),\dots,I^\gamma\vartheta_{2,M-1}(x),\ \dots,\ I^\gamma\vartheta_{2^{k-1},0}(x),\dots,I^\gamma\vartheta_{2^{k-1},M-1}(x)\right]^T. \tag{18}$$

To compute this matrix, we use the unit step function which is defined as follows:

$$\mu_c(x) = \begin{cases} 1, & x\ge c, \\ 0, & x<c. \end{cases}$$

In terms of the unit step function, we formulate Mittag-Leffler wavelets as follows:

$$\vartheta_{n,m}(x) = 2^{\frac{k-1}{2}}\left(\mu_{\frac{n-1}{2^{k-1}}}(x)\mathscr{M}_m\left(2^{k-1}x-n+1\right) - \mu_{\frac{n}{2^{k-1}}}(x)\mathscr{M}_m\left(2^{k-1}x-n+1\right)\right). \tag{19}$$

So

$$\vartheta_{n,m}(x) = \frac{2^{\frac{k-1}{2}}}{\sqrt{\int_0^1 ML_m^2(x)dx}}\left(\mu_{\frac{n-1}{2^{k-1}}}(x)ML_m\left(2^{k-1}x-n+1\right) - \mu_{\frac{n}{2^{k-1}}}(x)ML_m\left(2^{k-1}x-n+1\right)\right). \tag{20}$$

Utilizing the subsequent Laplace transform property

$$\mathscr{L}\{\mu_c(x)f(x)\} = e^{-cs}\mathscr{L}\{f(x+c)\}. \tag{21}$$

Then, we apply the Laplace transform to both sides of (20), that gives:

$$\begin{aligned}\mathscr{L}\{\vartheta_{n,m}(x)\} &= \frac{2^{\frac{k-1}{2}}}{\sqrt{\int_0^1 ML_m^2(x)dx}}\left(e^{-\frac{n-1}{2^{k-1}}s}\mathscr{L}\left\{ML_m\left(2^{k-1}x\right)\right\} - e^{-\frac{n}{2^{k-1}}s}\mathscr{L}\left\{ML_m\left(2^{k-1}x+1\right)\right\}\right)\\ &= \frac{2^{\frac{k-1}{2}}}{\sqrt{\int_0^1 ML_m^2(x)dx}}(e^{-\frac{n-1}{2^{k-1}}s}\mathscr{L}\left\{\sum_{k=0}^{n}\binom{n}{k}(n-1)_{n-k}2^k(2^{k-1}x)_k\right\}\\ &- e^{-\frac{n}{2^{k-1}}s}\mathscr{L}\left\{\sum_{k=0}^{n}\binom{n}{k}(n-1)_{n-k}2^k(2^{k-1}x+1)_k\right\}).\end{aligned} \tag{22}$$

According to (13), we have

$$(2^{k-1}x)_n = \sum_{l=0}^{n-1}\tilde{A}_l x^l, \qquad (2^{k-1}x+1)_n = \sum_{l=0}^{n-1}\tilde{B}_l x^l.$$

So, we get

$$\begin{aligned}\mathscr{L}\{\vartheta_{n,m}(x)\} &= \frac{2^{\frac{k-1}{2}}}{\sqrt{\int_0^1 ML_m^2(x)dx}}(e^{-\frac{n-1}{2^{k-1}}s}\sum_{k=0}^{n}\sum_{i=0}^{n-1}\binom{n}{k}(n-1)_{n-k}2^k\tilde{A}_i\mathscr{L}\{x^i\}\\ &-e^{-\frac{n}{2^{k-1}}s}\sum_{k=0}^{n}\sum_{i=0}^{n-1}\binom{n}{k}(n-1)_{n-k}2^k\tilde{B}_i\mathscr{L}\{x^i\}) = \frac{2^{\frac{k-1}{2}}}{\sqrt{\int_0^1 ML_m^2(x)dx}}\\ &\left(e^{-\frac{n-1}{2^{k-1}}s}\sum_{k=0}^{n}\sum_{i=0}^{n-1}\binom{n}{k}(n-1)_{n-k}2^k\tilde{A}_i\frac{i!}{s^{i+1}} - e^{-\frac{n}{2^{k-1}}s}\sum_{k=0}^{n}\sum_{i=0}^{n-1}\binom{n}{k}(n-1)_{n-k}2^k\tilde{B}_i\frac{\Gamma((i+1)!)}{s^{i+1}}\right)\\ &= \frac{2^{\frac{k-1}{2}}}{\sqrt{\int_0^1 ML_m^2(x)dx}}\sum_{k=0}^{n}\sum_{i=0}^{n-1}\binom{n}{k}(n-1)_{n-k}2^k\frac{i!}{s^{i+1}}\left(e^{-\frac{n-1}{2^{k-1}}s}\tilde{A}_i - e^{-\frac{n}{2^{k-1}}s}\tilde{B}_i\right).\end{aligned} \tag{23}$$

Based on Eq. (5), we obtain

$$\mathscr{L}\{I^\gamma\vartheta_{n,m}(x)\} = \frac{1}{\Gamma(\gamma)}\mathscr{L}\{x^{\gamma-1}\}\mathscr{L}\{\vartheta_{n,m}(x)\} = \frac{1}{s^\gamma}\mathscr{L}\{\vartheta_{n,m}(x)\}. \tag{24}$$

From (23) and (24), we get

$$\mathscr{L}\{I^\gamma\vartheta_{n,m}(x)\} = \frac{2^{\frac{k-1}{2}}}{\sqrt{\int_0^1 ML_m^2(x)dx}}\sum_{k=0}^{n}\sum_{i=0}^{n-1}\binom{n}{k}(n-1)_{n-k}2^k\frac{i!}{s^{i+1+\gamma}}\left(e^{-\frac{n-1}{2^{k-1}}s}\tilde{A}_i - e^{-\frac{n}{2^{k-1}}s}\tilde{B}_i\right). \tag{25}$$

Using the inverse Laplace transform from (25), we get

$$\begin{aligned}I^\gamma\vartheta_{n,m}(x) =& \frac{2^{\frac{k-1}{2}}}{\sqrt{\int_0^1 ML_m^2(x)dx}}\sum_{k=0}^{n}\sum_{i=0}^{n-1}\binom{n}{k}(n-1)_{n-k}2^k\frac{i!}{\Gamma(i+1+\gamma)}\\ &\left((x-\frac{n-1}{2^{k-1}})^{i+\gamma}\mu_{\frac{n-1}{2^{k-1}}}\tilde{A}_i - (x-\frac{n}{2^{k-1}})^{i+\gamma}\mu_{\frac{n}{2^{k-1}}}\tilde{B}_i\right).\end{aligned} \tag{26}$$

Therefore, by considering relation (26), we obtain

$$I^{\gamma}\vartheta_{n,m}(x)=\begin{cases}0, & x\in\left[0,\left(\frac{n-1}{2^{k-1}}\right)\right),\\ \theta(x), & x\in\left[\left(\frac{n-1}{2^{k-1}}\right),\left(\frac{n}{2^{k-1}}\right)\right),\\ \theta(x)-\tilde{\theta}(x), & x\in\left[\left(\frac{n}{2^{k-1}}\right),1\right),\end{cases}\tag{27}$$

where

$$\theta(x)=\frac{2^{\frac{k-1}{2}}}{\sqrt{\int_0^1 ML_m^2(x)dx}}\sum_{k=0}^{n}\sum_{i=0}^{n-1}\left(\begin{array}{c}n\\k\end{array}\right)(n-1)_{n-k}2^k\frac{i!}{\Gamma(i+1+\gamma)}(x-\frac{n-1}{2^{k-1}})^{i+\gamma}\tilde{A}_i,\tag{28}$$

and

$$\tilde{\theta}(x)=\frac{2^{\frac{k-1}{2}}}{\sqrt{\int_0^1 ML_m^2(x)dx}}\sum_{k=0}^{n}\sum_{i=0}^{n-1}\left(\begin{array}{c}n\\k\end{array}\right)(n-1)_{n-k}2^k\frac{i!}{\Gamma(i+1+\gamma)}(x-\frac{n}{2^{k-1}})^{i+\gamma}\tilde{B}_i.\tag{29}$$

To clarify the construction of $\tilde{\vartheta}(x,\gamma)$, consider a simple case with $k=2$ and $M=2$. The fractional integral of order $\gamma=\frac{1}{2}$ can be computed as:

$$\tilde{\vartheta}(x,\frac{1}{2})=\begin{bmatrix}2\sqrt{\frac{2}{\pi}}\left(\sqrt{x}-\sqrt{-\frac{1}{2}+x}H(-\frac{1}{2}+x)\right)\\ \sqrt{\frac{2}{3\pi}}\left(8x^{3/2}-\sqrt{-2+4x}(1+4x)H(-\frac{1}{2}+x)\right)\\ \frac{1}{3}\sqrt{\frac{2}{5\pi}}\left(64x^{5/2}-\sqrt{-2+4x}(3+8x(1+4x))H(-\frac{1}{2}+x)\right)\\ \sqrt{\frac{2}{\pi}}\left(-2\sqrt{-1+x}H(-1+x)+\sqrt{-2+4x}H(-\frac{1}{2}+x)\right)\\ 2\sqrt{\frac{2}{3\pi}}\left((1-4x)\sqrt{-1+x}H(-1+x)+\sqrt{2}(-1+2x)^{3/2}H(-\frac{1}{2}+x)\right)\\ \frac{2}{3}\sqrt{\frac{2}{5\pi}}\left(\sqrt{-1+x}(-7+8(3-4x)x)H(-1+x)+4\sqrt{2}(-1+2x)^{5/2}H(-\frac{1}{2}+x)\right)\end{bmatrix},$$

where $H(x)$ denotes the Heaviside step function, and each entry represents the fractional integral of the corresponding Mittag-Leffler wavelet.

3 Numerical method

In this article, we provide a computational approach for finding approximate solution of the following problems.

Problem 1. PDDEs:

We assume that

$$D^{\nu}u(t)\simeq C^{\mathrm{T}}\vartheta(x).\tag{30}$$

We get

$$u(x)\simeq I^{\nu}\left(C^{\mathrm{T}}\vartheta(x)\right)+\sum_{i=0}^{n-1}\frac{p_i}{i!}x^i\simeq C^{\mathrm{T}}\tilde{\vartheta}(x,\gamma)+\sum_{i=0}^{n-1}\frac{p_i}{i!}x^i,\tag{31}$$

and

$$u(\tau x)\simeq I^{\nu}\left(C^{\mathrm{T}}\vartheta(\tau x)\right)+\sum_{i=0}^{n-1}\frac{p_i}{i!}\tau^i x^i\simeq C^{\mathrm{T}}\tilde{\vartheta}(\tau x,\gamma)+\sum_{i=0}^{n-1}\frac{p_i}{i!}\tau^i x^i.\tag{32}$$

By substituting Eqs. (30)-(32) into (1), the resulting equation is collocated at the chosen points

$$x_i = \frac{2i-1}{2^{k-1}(M+1)}, \quad i = 1,2,\ldots,2^{k-1}(M+1).$$

This procedure leads to a system of $2^{k-1}(M+1)$ algebraic equations for $2^{k-1}(M+1)$ unknown coefficients c_n. The resulting nonlinear system can be solved using Newton's iteration method. Once the coefficients are obtained, substituting them into Eq. (31) provides an approximate solution to the original problem.

Problem 2. Time- fractional partial PDDEs: To numerically solve time-fractional PDDEs, we can expand $\frac{\partial^3 u}{\partial x^2 \partial t}$ in the following manner:

$$\frac{\partial^3 u}{\partial x^2 \partial t} \simeq (\vartheta(x))^T \mathbf{U} \vartheta(t). \tag{33}$$

Using the initial condition, we integrate Eq. (33) with respect to t, yielding the following result:

$$\frac{\partial^2 u}{\partial x^2} \simeq (\vartheta(x))^T \mathbf{U} \tilde{\vartheta}(t,1) + \phi''(x), \tag{34}$$

where $\tilde{\vartheta}(t,1)$ is the operational integration matrix corresponding to t. Moreover, by integrating the previous equation with respect to x, we get

$$\frac{\partial u}{\partial x} \simeq (\tilde{\vartheta}(x,1))^T \mathbf{U} \tilde{\vartheta}(t,1) + (\phi'(x) - \phi'(0)) + \frac{\partial u(0,t)}{\partial x}, \tag{35}$$

in which $\frac{\partial u(0,t)}{\partial x}$ is unknown. The following relation is determined by integrating Eq. (35) with respect to x:

$$u(x,t) \simeq \tilde{\vartheta}(x,2))^T \mathbf{U} \tilde{\vartheta}(t,1) + (\phi(x) - \phi(0) - x\phi'(0)) + x\frac{\partial u(0,t)}{\partial x} + \psi_0(t). \tag{36}$$

We integrate Eq. (36) with respect to x from 0 to 1 in order to calculate $\frac{\partial u(0,t)}{\partial x}$. Subsequently, we obtain

$$\psi_1(t) - \psi_0(t) = \left(\int_0^1 (\tilde{\vartheta}(x,2))^T dx \right) \mathbf{U} \tilde{\vartheta}(t,1) + (\phi(1) - \phi(0) - \phi'(0)) + \frac{\partial u(0,t)}{\partial x}. \tag{37}$$

Then

$$\frac{\partial u(0,t)}{\partial x} = \psi_1(t) - \psi_0(t) - \left(\int_0^1 (\tilde{\vartheta}(x,2))^T dx \right) \mathbf{U} \tilde{\vartheta}(t,1) - (\phi(1) - \phi(0) - \phi'(0)). \tag{38}$$

Hence, the approximation of $u(x,t)$ is obtained using Eqs. (36), (38). By performing two integrations of Eq. (33) with respect to x, we can determine $\frac{\partial u(x,t)}{\partial t}$, as follows:

$$\frac{\partial u(x,t)}{\partial t} \simeq (\tilde{\vartheta}(x,2))^T \mathbf{U} \vartheta(t) + \psi_0'(t). \tag{39}$$

Next, we approximate the value of $\frac{\partial^\gamma u(x,t)}{\partial t^\gamma}$ as

$$\frac{\partial^\gamma u(x,t)}{\partial t^\gamma} \simeq I_t^{1-\gamma} \left(\frac{\partial u(x,t)}{\partial t} \right) = (\tilde{\vartheta}(x,2))^T \mathbf{U} \tilde{\vartheta}(t,1-\gamma) + I^{1-\gamma}(\psi_0'(t)). \tag{40}$$

By replacing the aforementioned approximations in the governing equation, this leads to an algebraic equation. We then apply the collocation method at the following nodal points:

$$x_i = \frac{2i-1}{2^k(M+1)}, \quad t_j = \frac{2j-1}{2^k(M+1)}, \quad i,j = 1,2,\ldots,2^{k-1}M. \tag{41}$$

Subsequently, we solve the problem using Newton's iterative method and obtain the approximate solution by calculating the coefficients.

4 Error examination

This section focuses on demonstrating the convergence of the numerical approximation to the exact solution.

Theorem 1. *([14]) Assume that $U \in H^{\omega}(0,1)$ for $\omega \geq 0$, and let $\tilde{U}$ represent the best approximation to U. Then the following holds:*

$$\|U-\tilde{U}\|_{L^2(0,1)} \leq c(M-1)^{-\omega}\left\|U^{(\omega)}\right\|_{L^2(0,1)}. \tag{42}$$

In addition, for $\iota \geq 1$, we obtain following:

$$\|U-\tilde{U}\|_{H^{\iota}(0,1)} \leq c(M-1)^{2\iota-\frac{1}{2}-\omega}\left\|y^{(\omega)}\right\|_{L^2(0,1)}. \tag{43}$$

Theorem 2. *Suppose $U \in H^{\omega}(0,1)$ with $\omega \geq 0$, and let $0 \leqslant \gamma < 1$ and $0 \leqslant \iota < \omega$. Then*

$$\left\|D^{\gamma}U - D^{\gamma}\tilde{U}\right\|_{L^2(0,1)} \leq \frac{1}{\Gamma(2-\gamma)}\mathrm{c}(M-1)^{2\iota-\frac{1}{2}-\omega}\left\|U^{(\omega)}\right\|_{L^2(0,1)}. \tag{44}$$

Proof. The relationship between the RLFI and the Caputo fractional derivative is given by the following identity:

$$D^{\gamma}U(x) = I^{n-\gamma}D^{n}U(x).$$

Utilizing Eqs. (42) and (43) together with the aforementioned relation for $n=1$, we obtain

$$\|U*Z\|_p \leq \|U\|_1\|Z\|_p,$$

so

$$\begin{aligned}
\left\|D^{\gamma}U - D^{\gamma}\tilde{U}\right\|^2_{L^2(0,1)} &= \left\|I_x^{1-\gamma}\left(D^1U(x) - D^1\tilde{U}(x)\right)\right\|^2_{L^2(0,1)} \\
&= \left\|\frac{1}{x^{\gamma}\Gamma(1-\gamma)} * \left(D^1U(x) - D^1\tilde{U}(x)\right)\right\|^2_{L^2(0,1)} \\
&\leq \left(\frac{1}{(1-\gamma)\Gamma(1-\gamma)}\right)^2 \left\|D^1U(x) - D^1\tilde{U}(x)\right\|^2_{L^2(0,1)} \\
&\leq \left(\frac{1}{\Gamma(2-\gamma)}\right)^2 \|U(x)-\tilde{U}(x)\|^2_{H^{\iota}(0,1)} \\
&\leq \left(\frac{1}{\Gamma(2-\gamma)}\right)^2 c^2(M-1)^{4\iota-1-2\omega}\left\|U^{(\omega)}\right\|^2_{L^2(0,1)}.
\end{aligned} \tag{45}$$

□

Theorem 3. *Let $U \in H^{\omega}(0,1)$ with $\omega \geq 0$, and suppose $M \geq \iota$, then the following result is obtained*

$$\left\|D^{\xi(\gamma)}U - D^{\xi(\gamma)}\tilde{U}\right\|_{L^2(0,1)} \leq \Omega c(M-1)^{2\iota-\frac{1}{2}-\omega} \times \left\|U^{(\omega)}\right\|_{L^2(0,1)}, \tag{46}$$

where

$$\|\xi(\gamma)\|_{L^2(0,1)} \leq \omega.$$

Proof. Let us consider that

$$\begin{aligned}\left\|D^{\xi(\gamma)}U-D^{\xi(\gamma)}\tilde{U}\right\|_{L^2(0,1)}&=\left\|\int_0^1\xi(\gamma)\left(\|D^{\gamma}U(x)-D^{\gamma}\tilde{U}(x)\right)\mathrm{d}\gamma\right\|_{L^2(0,1)}\\&\leq\int_0^1\|\xi(\gamma)\|_{L^2(0,1)}\left\|D^{\gamma}U(x)-D^{\gamma}\tilde{U}(x)\right\|_{L^2(0,1)}\mathrm{d}\gamma\\&\leq\int_0^1\Omega\left(\frac{1}{\Gamma(2-\gamma)}c(M-1)^{2\iota-\frac{1}{2}-\omega}\left\|U^{(\omega)}\right\|_{L^2(0,1)}\right)\mathrm{d}\gamma\\&\leq\Omega c(M-1)^{2\iota-\frac{1}{2}-\omega}\left\|U^{(\omega)}\right\|_{L^2(0,1)}.\end{aligned}\tag{47}$$

□

5 Examples

In this section, we present the results of test problems to display the accuracy and effectiveness of the suggested numerical schemes.

Example 1. We consider the following pantograph model problem:

$$D^{(\gamma)}u(x)+u(x)+\left(D^{(\gamma)}u(\frac{1}{3}x)\right)^3=u(\frac{x}{2})+\frac{8}{27}x^3+\frac{3}{4}x^2+2x,\quad 0<\gamma\leq 1.\tag{48}$$

The initial condition is $u(0)=0$ and the exact solution is $u(x)=x^2$, for $\gamma=1$. To solve this problem, we apply the current technique. The exact and approximate solution of various values of $\gamma=0.5,0.6,...,1$ are shown in Fig. 1. The graphs of absolute errors for $\gamma=1$ and $M=k=2$ are shown in Fig. 2. The results shown in these figures demonstrate that even a small number of Mittag-Leffler wavelet terms provide a close approximation to the exact solution.

Example 2. Consider the nonlinear singular fractional differential equations with proportional delay

$$D^{(\gamma)}u(x)=-u(x)+(\frac{1}{2})u(\frac{1}{2}x)+cos(x)+sin(x)-\frac{1}{2}sin(\frac{1}{2}x),\quad 0<\gamma\leq 1,\tag{49}$$

where $u(0)=0$. When $\gamma=1$, the exact solution is $u(x)=sin(x)$. Fig. 3 shows an approximation and its absolute error with parameters $k=2, M=4$. Table 1 compares our results to the achieved result using the Bernoulli wavelet approach [22] with $k=2, M=6$, and the Legendre wavelet method [28] with $k=2, M=6$. The last two columns provide the percentage improvement achieved by our approach. According to the theoretical error bound (47), one obtains

$$\|D^{\gamma}U-D^{\gamma}\tilde{U}\|_{L^2(0,1)}\leq 0.21c.$$

This estimate provides a conservative upper bound, whereas the numerical results in Table 1 are of the order of 10^{-12}. Hence, the practical accuracy of the proposed method substantially surpasses the theoretical guarantee, demonstrating the robustness and effectiveness of the approach.

Example 3. This example focuses on the analysis of a linear multi-PDDEs with delay as follows:

$$D^{(\gamma)}u(x)=-u(x)-e^{-\frac{1}{2}x}sin(\frac{1}{2}x)u(\frac{1}{2}x)-2e^{-\frac{3}{4}x}cos(\frac{1}{2}x)sin(\frac{1}{4}x)u(\frac{1}{4}x),\quad 0<\gamma\leq 1.\tag{50}$$

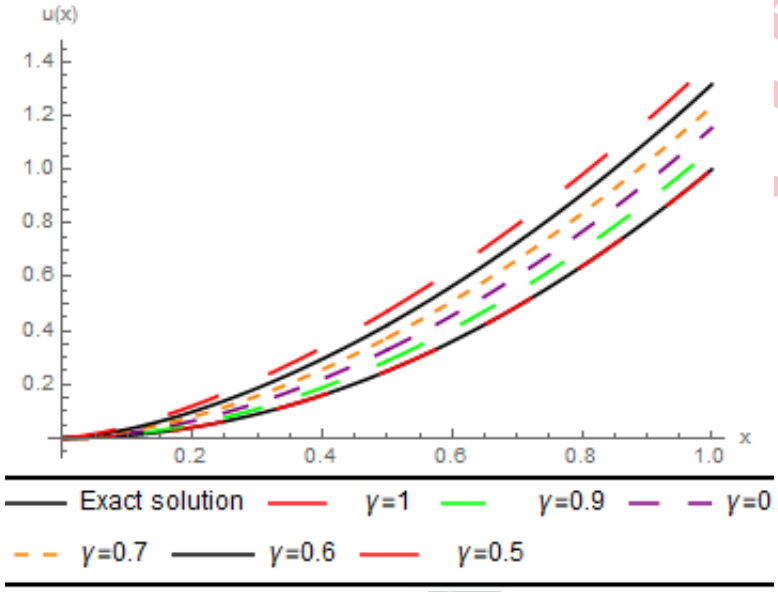

Figure 1: The computed solutions using $M = k = 2$, diverse $\gamma = 0.5, 0.6, ..., 0.9$ and 1 in Example 1

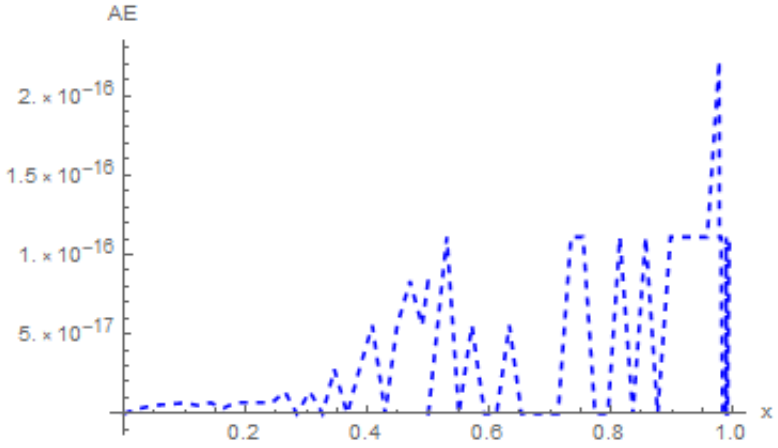

Figure 2: The absolute errors for Example 1 when $k = 2$, $M = 2$ and $\gamma = 1$

Table 1: Comparison of absolute errors of the proposed method for $\gamma = 1$, with Bernoulli and Legendre wavelet methods for Example 2, along with the percent improvement of the proposed method

x	Absolute errors			Percent improvement of our method	
	Bernoulli $k = 2, M = 6$	**Legendre wavelet** $k = 2, M = 6$	**Our method** $k = 2, M = 6$	**vs Bernoulli (%)**	**vs Legendre (%)**
0	5.93×10^{-9}	0	0	100	0
0.2	2.27×10^{-10}	7.82×10^{-10}	3.83×10^{-12}	98.31	99.51
0.4	1.22×10^{-9}	7.02×10^{-10}	3.08×10^{-12}	99.75	99.56
0.6	5.57×10^{-6}	1.94×10^{-9}	8.45×10^{-12}	99.9998	99.56
0.8	4.56×10^{-6}	1.64×10^{-9}	8.18×10^{-12}	99.9998	99.50

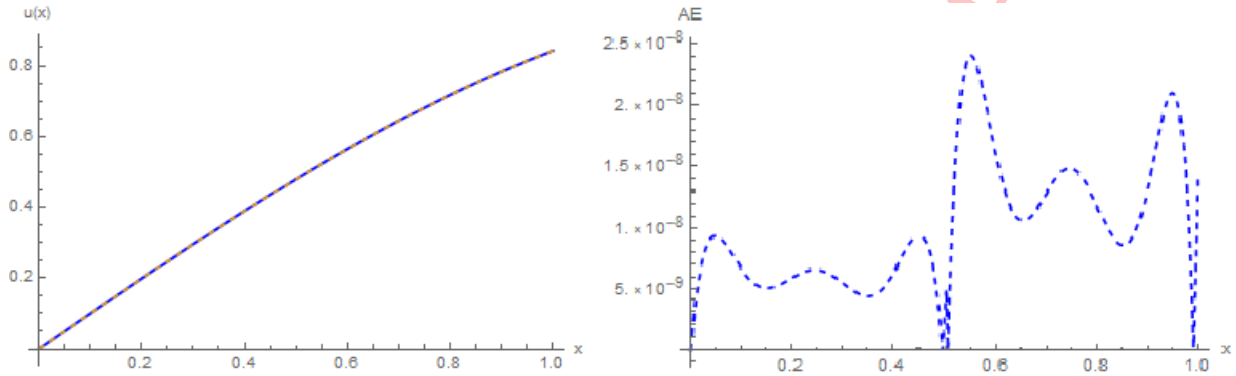

Figure 3: In the left graph, the exact solution (solid line) is compared with the approximate solution (dots), whereas the right graph displays the absolute error associated with Example 2 using $k = 2$, $M = 4$ and $\gamma = 1$

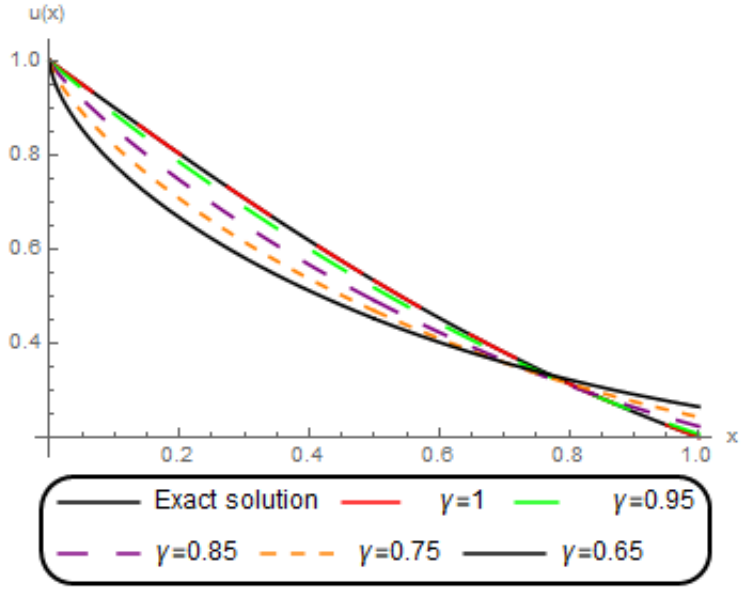

Figure 4: Approximate solutions obtained using the proposed method with $k = 2$, $M = 4$, illustrating the effect of varying γ in Example 3

The equation is considered with the initial condition $u(0) = 1$, and its exact solution is $e^{-x}cos(x)$. Fig. 4 illustrates the numerical results for $M = 4$, $k = 2$ under varying values of γ, in comparison with the analytical solution. The results clearly demonstrate that as $\gamma \longrightarrow 1$, the numerical solutions increasingly aligns with the exact solution. Furthermore, Fig. 5 illustrates the absolute error plots of the proposed numerical scheme. Overall, the figures confirm that the proposed scheme achieves a high degree of accuracy, closely approximating the analytical solution.

Example 4. We now examine a nonlinear singular fractional PDDEs of the form:

$$x^2 D^{(\gamma)} u(x) = x^2 u(x) - 8(u(\frac{1}{2}x))^2, \quad 1 < \gamma \leq 2, \tag{51}$$

The problem is considered with initial conditions $u(0) = 0$, and $\acute{u}(0) = 1$. For $\gamma = 2$, the differential equation admits the exact solution $u(x) = xe^{-x}$. Table 2 reports the absolute errors associated with the numerical solutions

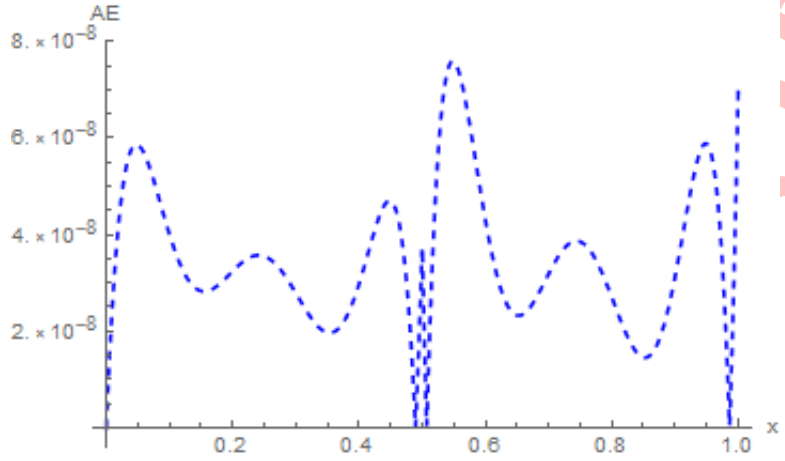

Figure 5: The absolute errors for Example 3 when $k = 2$, $M = 4$ and $\gamma = 1$

obtained via the proposed method and the Gegenbauer wavelet step method [10], for $k = 1$ and $M = 5$ and $M = 8$. The additional columns present the computed percentage improvements. The data clearly demonstrate that the proposed method achieves higher accuracy in comparison to the Gegenbauer wavelet step method.

Table 2: Comparison of absolute errors of the present method for $\gamma = 2$, with the Gegenbauer wavelet method for Example 4, along with the percent improvement of the proposed method

x	$k = 1, M = 5$			$k = 1, M = 8$		
	Method in [10]	Present Method	Improvement (%)	Method in [10]	Present Method	Improvement (%)
0.0	1.56×10^{-15}	0	100	1.54×10^{-16}	0	100
0.1	1.35×10^{-6}	5.37×10^{-8}	96.02	6.73×10^{-10}	4.87×10^{-12}	99.28
0.2	1.90×10^{-5}	9.94×10^{-8}	99.48	3.32×10^{-10}	8.02×10^{-12}	97.58
0.3	3.72×10^{-5}	1.15×10^{-7}	99.69	1.29×10^{-9}	9.57×10^{-12}	99.26
0.4	2.42×10^{-5}	1.18×10^{-7}	99.51	1.12×10^{-9}	9.66×10^{-12}	99.14
0.5	2.99×10^{-5}	1.08×10^{-7}	99.64	3.14×10^{-9}	8.54×10^{-12}	99.73
0.6	8.12×10^{-5}	7.95×10^{-8}	99.90	3.72×10^{-9}	6.38×10^{-12}	99.83
0.7	1.94×10^{-6}	3.33×10^{-8}	98.28	7.44×10^{-9}	4.88×10^{-12}	99.93
0.8	4.45×10^{-4}	1.95×10^{-9}	99.9996	1.52×10^{-8}	4.59×10^{-13}	99.997
0.9	1.63×10^{-3}	5.80×10^{-8}	99.996	4.36×10^{-8}	4.96×10^{-12}	99.89

Example 5. We consider the following fractional PDDEs:

$$D^{(\gamma)}u(x) = -u(x) + \frac{1}{2}u\left(\tfrac{x}{2}\right) + \frac{\Gamma(\alpha+1)}{\Gamma(\alpha+1-\gamma)}x^{\alpha-\gamma} + x^{\alpha} - \frac{1}{2^{\alpha+1}}x^{\alpha}, \quad 0 < \gamma \leq 1, \tag{52}$$

subject to the initial condition $u(0) = 0$. The exact solution is $u(x) = x^{\alpha}$ with $0 < \alpha < 1$. For the numerical experiments, we set $\alpha = \frac{1}{2}$ and $\gamma = \frac{1}{2}$.

This example is particularly challenging since the exact solution is continuous but exhibits an unbounded derivative near $x = 0$. Therefore, it serves as a strong benchmark for testing the stability and convergence of the proposed numerical method.

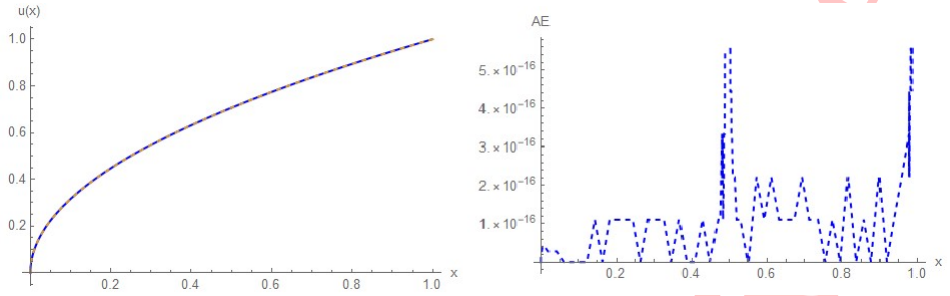

Figure 6: Left: exact solution (solid line) versus numerical approximation (dots). Right: absolute error for Example 5 with $k = 2$, $M = 6$, and $\gamma = \frac{1}{2}$

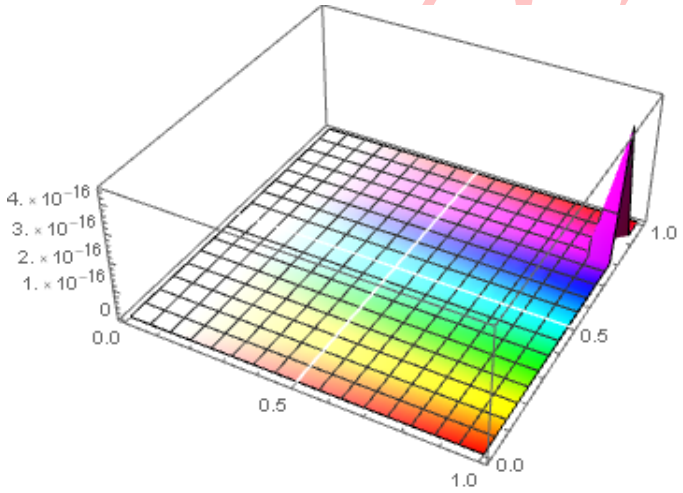

Figure 7: Absolute error for Example 6 with $k = 2$, $M = 2$, and $\gamma = 1$

Fig. 6 compares the numerical solution obtained with our Mittag-Leffler wavelet collocation method ($k = 2$, $M = 6$) against the exact solution (left) and its absolute error (right). The results confirm that our approach successfully resolves the boundary singularity and achieves good accuracy throughout the computational domain.

Example 6. Consider the nonlinear time-fractional Burgers equation with proportional delay:

$$D_t^{\gamma} u(x,t) = \frac{\partial^2}{\partial x^2} u(x,t) + \frac{\partial}{\partial x} u\left(x, \frac{t}{2}\right) u\left(\frac{x}{2}, \frac{t}{2}\right) + \frac{1}{2} u(x,t), \quad 0 < \gamma \leq 1,\ x,t \in [0,1], \tag{53}$$

with the initial condition $u(x,0) = x$. For $\gamma = 1$, the exact solution is $u(x,t) = x e^t$.

Numerical results demonstrate the effectiveness of the proposed method. Fig. 7 illustrate the absolute error on $[0,1] \times [0,1]$. Comparison with previous methods indicates that the present approach achieves higher accuracy, showing that it is a reliable and efficient technique for solving this fractional Burgers equation with proportional delay. Table 3 demonstrates the absolute errors of approximate solutions for $M = k = 2$, $\gamma = 1$. Compared to the Genocchi hybrid method [2], the proposed method with $m = k = 2$ yields significantly smaller absolute errors, demonstrating its accuracy.

The numerical results demonstrate that the proposed Mittag-Leffler wavelet method not only effectively handles problems with unbounded derivatives near the boundaries, but also achieves higher accuracy compared to

Table 3: Comparison of absolute errors obtained by the Genocchi–hybrid method and the proposed method on the interval $[0,1]$

(x,t)	Genocchi hybrid [2] $(N=1, M_1=2, M_2=9)$	Genocchi hybrid [2] $(N=2, M_1=2, M_2=9)$	Proposed method $(m=k=2)$
(0,0)	0	0	0
(0.1,0.1)	4.56×10^{-8}	3.40×10^{-8}	5.49×10^{-20}
(0.2,0.2)	8.08×10^{-8}	5.45×10^{-8}	2.43×10^{-20}
(0.3,0.3)	1.15×10^{-7}	7.28×10^{-8}	6.80×10^{-19}
(0.4,0.4)	1.60×10^{-7}	1.01×10^{-7}	7.88×10^{-19}
(0.5,0.5)	2.25×10^{-7}	2.53×10^{-7}	2.10×10^{-18}
(0.6,0.6)	3.23×10^{-7}	3.13×10^{-6}	5.32×10^{-18}
(0.7,0.7)	4.64×10^{-7}	3.32×10^{-6}	4.20×10^{-18}
(0.8,0.8)	6.63×10^{-7}	3.57×10^{-6}	6.29×10^{-18}
(0.9,0.9)	9.31×10^{-7}	3.88×10^{-6}	2.55×10^{-17}
(1,1)	1.28×10^{-6}	4.24×10^{-6}	0

existing methods. Moreover, the numerical implementation requires relatively fewer computations, indicating a significant advantage in computational efficiency. These characteristics underscore the main novelty of the proposed approach compared to other similar techniques.

6 Conclusion

In this study, we developed an efficient and accurate approximate solution method for PDDEs with delays by employing Mittag-Leffler wavelet functions. We formulated the RLFI operator associated with these wavelets and, using a collocation strategy, transformed the original fractional differential equations into solvable algebraic systems. The proposed method provides a systematic and computationally efficient framework, particularly effective for addressing the challenges posed by delays and singularities in pantograph-type problems. Through multiple numerical examples, we have demonstrated the method's high accuracy and reliability, with the approximate solutions showing excellent agreement with exact solutions and existing wavelet-based approaches. The proposed technique offers practical benefits, including systematic handling of delays and singularities, computational efficiency, and applicability to complex pantograph-type problems. For future work, the method can be extended to multi-dimensional fractional systems and adaptive strategies can be explored to further improve accuracy and efficiency.

A Existence and uniqueness of the solution

Prior to constructing a numerical scheme, it is crucial to establish that the fractional PDDEs (1) is well-posed, i.e., it admits a unique solution. We approach this by reformulating the problem into an equivalent integral equation framework and employing fixed-point theory under appropriate Lipschitz-type conditions, following the standard methodology for such analyses [19]. A similar framework has also been recently adopted for fractional problems with delays in [25], confirming the suitability of this approach.

Theorem 4 (Equivalent Integral Formulation)**.** *Let $n-1<\gamma\le n$. The fractional PDDEs (1) subject to the initial conditions $u^{(s)}(0)=p_s$, for $s=0,1,...,n-1$, is equivalent to the following nonlinear Volterra integral equation:*

$$u(x)=\sum_{i=0}^{n-1}\frac{p_i}{i!}x^i+\frac{1}{\Gamma(\gamma)}\int_0^x(x-s)^{\gamma-1}\left[a_0(s)u(s)+\sum_{l=1}^{L}a_l(s)D^{\eta_l}u(\tau_l s)+\chi(s)\right]ds. \tag{54}$$

Proof. The proof follows directly by applying the Riemann–Liouville fractional integral operator I^γ to both sides of Eq. (1) and utilizing the inverse property $I^\gamma D^\gamma u(x)=u(x)-\sum_{i=0}^{n-1}u^{(i)}(0)\frac{x^i}{i!}$ (see Eq. (8)). □

To facilitate the analysis, we define an operator $\mathscr{T}$ on a suitable function space. Let $\mathscr{X}=C[0,1]$ be the Banach space of continuous functions on $[0,1]$ equipped with the supremum norm $\|u\|_\infty=\sup_{x\in[0,1]}|u(x)|$. We define the operator $\mathscr{T}:\mathscr{X}\to\mathscr{X}$ by

$$(\mathscr{T}u)(x)=\sum_{i=0}^{n-1}\frac{p_i}{i!}x^i+I^\gamma\left[a_0(\cdot)u(\cdot)+\sum_{l=1}^{L}a_l(\cdot)D^{\eta_l}u(\tau_l\cdot)+\chi(\cdot)\right](x). \tag{55}$$

A fixed point of this operator, $u=\mathscr{T}u$, is a solution to the integral equation and hence to the original problem (1).

Assumption 1. *The known functions $a_l(x)$ $(l=0,1,...,L)$ and $\chi(x)$ are continuous on $[0,1]$. Assume further that the exact solution u lies in a Sobolev space $H^\omega(0,1)$ with $\omega>\max_l\gamma_l$. Under this condition, the fractional derivatives $D^{\eta_l}u$ exist in L^2 and the nonlinear forcing term satisfies a Lipschitz condition; there exists a constant $K>0$ such that*

$$\left|a_0(x)u(x)+\sum_{l=1}^{L}a_l(x)D^{\eta_l}u(\tau_l x)-\left(a_0(x)v(x)+\sum_{l=1}^{L}a_l(x)D^{\eta_l}v(\tau_l x)\right)\right|\le K\|u-v\|_\infty \tag{56}$$

for any $u,v\in\mathscr{X}$ and for all $x\in[0,1]$.

Theorem 5 (Existence and Uniqueness)**.** *Under Assumption 1, the operator $\mathscr{T}$ is a contraction on $\mathscr{X}$ for a sufficiently small interval $[0,\delta]\subset[0,1]$. Consequently, by the Banach Fixed-Point Theorem, the integral equation and thus the fractional pantograph problem (1) has a unique solution $u^*\in C[0,\delta]$. This directly establishes that the problem is well posed in the sense of Hadamard.*

Proof. Let $u,v\in\mathscr{X}$. We estimate the distance between $\mathscr{T}u$ and $\mathscr{T}v$:

$$\begin{aligned}|(\mathscr{T}u)(x)-(\mathscr{T}v)(x)|&\le\frac{1}{\Gamma(\gamma)}\int_0^x(x-s)^{\gamma-1}K\|u-v\|_\infty ds\quad\text{(by Assumption 1)}\\&=\frac{K}{\Gamma(\gamma+1)}x^\gamma\|u-v\|_\infty.\end{aligned}$$

Taking the supremum over $x\in[0,\delta]$, we get

$$\|\mathscr{T}u-\mathscr{T}v\|_\infty\le\frac{K\delta^\gamma}{\Gamma(\gamma+1)}\|u-v\|_\infty.$$

Choosing $\delta>0$ such that $L^*=\frac{K\delta^\gamma}{\Gamma(\gamma+1)}<1$, the operator $\mathscr{T}$ becomes a contraction on $C[0,\delta]$. The Banach Fixed-Point Theorem then guarantees the existence of a unique fixed point $u^*\in C[0,\delta]$. This local solution can be extended to the entire interval $[0,1]$ using standard continuation arguments [19]. □

Corollary 1. *For the linear case of problem (1), the solution exists and is unique on the entire interval $[0,1]$. In this setting, the Lipschitz constant K can be chosen independent of the interval length, and thus the well-posedness is guaranteed globally without the need for stepwise continuation.*

B Convergence and stability analysis

In this section, we provide a rigorous convergence and stability analysis for the proposed Mittag-Leffler wavelet collocation method applied to the fractional PDDEs given in Eq. (1). We establish uniform error bounds in the L^∞-norm and demonstrate the stability of the numerical scheme.

B.1 Preliminaries and assumptions

Let $u(x)$ be the exact solution of the fractional PDDEs and $\tilde{u}(x)$ be the approximate solution obtained by the proposed method. We assume that $u \in H^\omega([0,1])$ for some $\omega \geq 1$, where H^ω denotes the Sobolev space of order ω. This implies that the derivatives of u up to order ω are bounded in $L^\infty([0,1])$.

The Mittag-Leffler wavelet approximation space is defined as

$$V_M = \text{span}\{\vartheta_{n,m}(x) : 1 \leq n \leq 2^{k-1}, 0 \leq m \leq M-1\},$$

where M represents the number of basis functions. Let $\Pi_M : H^\omega([0,1]) \to V_M$ be the projection operator onto the wavelet space V_M.

B.2 Projection error estimate

Lemma 1 (Projection Error)**.** *Suppose $u \in H^\omega([0,1])$ with $\omega \geq 1$. Then, there exists a constant C independent of M such that*

$$\|u - \Pi_M u\|_{L^\infty([0,1])} \leq CM^{-(\omega-1)} \|u^{(\omega)}\|_{L^\infty([0,1])}.$$

Proof. The proof follows from the approximation properties of Mittag-Leffler wavelets. The basis functions $\vartheta_{n,m}$ form a complete system in $L^2([0,1])$, and their approximation properties are well-established [7]. Using the Sobolev Embedding Theorem and the fact that the wavelets capture polynomial behavior up to degree $M-1$, we obtain the stated estimate. The constant C depends on the wavelet basis but not on M. □

B.3 Residual estimate

Lemma 2 (Residual Estimate)**.** *The residual term satisfies*

$$\|R_M\|_{L^\infty([0,1])} \leq CM^{-(\omega-1)} \|u^{(\omega)}\|_{L^\infty([0,1])},$$

where C is a constant independent of M.

Proof. The residual arises from two sources: (i) the approximation of u by $\Pi_M u$, and (ii) the numerical discretization of the fractional operator. Using the Lipschitz continuity of the fractional integral operator and the boundedness of the coefficients $a_l(x)$, we have:

$$|R_M(x)| \leq |D^\gamma(u - \Pi_M u)(x)| + |a_0(x)(u - \Pi_M u)(x)| + \sum_{l=1}^{L} |a_l(x) D^{\eta}(u - \Pi_M u)(\tau_l x)|.$$

From the boundedness of $a_l(x)$ and the estimate $\|D^\gamma(u - \Pi_M u)\|_{L^\infty} \leq C\|u - \Pi_M u\|_{L^\infty}$, we obtain:

$$\|R_M\|_{L^\infty} \leq C\|u - \Pi_M u\|_{L^\infty}.$$

Applying Lemma 1 completes the proof. □

B.4 Stability Analysis

Theorem 6 (Stability). *The numerical scheme defined by the Mittag-Leffler wavelet collocation method is stable. Specifically, there exists a constant C, independent of M, such that for any function $v \in V_M$, the following inequality holds:*

$$\|v\|_{L^\infty([0,1])} \leq C \left(\|D^\gamma v\|_{L^\infty([0,1])} + \sum_{l=1}^{L} \|D^{\eta_l} v(\tau_l \cdot)\|_{L^\infty([0,1])} + \|v\|_{L^\infty(\partial\Omega)} \right),$$

where $\partial\Omega$ represents the boundary conditions.

Proof. The stability is established by constructing a suitable energy estimate. Consider the discrete operator $\mathscr{L}_M$ defined by:

$$\mathscr{L}_M v = D^\gamma v - a_0(x)v - \sum_{l=1}^{L} a_l(x) D^{\eta_l} v(\tau_l x).$$

Using the discrete maximum principle for fractional differential equations [19], we can show that the operator $\mathscr{L}_M$ is uniformly stable. The boundedness of the coefficients $a_l(x)$ and the approximation properties of the Mittag-Leffler wavelet basis guarantee that the system matrix is diagonally dominant for sufficiently fine discretizations. Therefore, there exists a constant C, depending only on the coefficients and fractional order γ (but not on M), such that:

$$\|v\|_{L^\infty} \leq C \|\mathscr{L}_M v\|_{L^\infty}.$$

The boundary terms appear when applying the maximum principle, leading to the stated inequality. □

B.5 Convergence Analysis

Theorem 7 (Uniform Convergence). *Let u be the exact solution of (1) and $\tilde{u}$ be the numerical solution obtained by the proposed Mittag-Leffler wavelet method. Then, there exists a constant C independent of M such that:*

$$\|u - \tilde{u}\|_{L^\infty([0,1])} \leq C M^{-(\omega-1)} \|u^{(\omega)}\|_{L^\infty([0,1])}.$$

Proof. Using the error decomposition:

$$\|u - \tilde{u}\|_{L^\infty} \leq \|u - \Pi_M u\|_{L^\infty} + \|\Pi_M u - \tilde{u}\|_{L^\infty},$$

the first term is bounded by Lemma 1. For the second term, we use the stability result (Theorem 6). Note that $\Pi_M u - \tilde{u} \in V_M$ and satisfies:

$$\mathscr{L}_M(\Pi_M u - \tilde{u}) = R_M.$$

Applying Theorem 6 yields:

$$\|\Pi_M u - \tilde{u}\|_{L^\infty} \leq C \|R_M\|_{L^\infty}.$$

Finally, using Lemma 2 to bound $\|R_M\|_{L^\infty}$, we obtain:

$$\|\Pi_M u - \tilde{u}\|_{L^\infty} \leq C M^{-(\omega-1)} \|u^{(\omega)}\|_{L^\infty}.$$

Combining both error estimates completes the proof. □

B.6 Discussion

The analysis demonstrates that the proposed method converges uniformly with order $\mathcal{O}(M^{-(\omega-1)})$. The use of the L^∞-norm provides a stronger result than L^2-based estimates, since it ensures pointwise convergence and directly addresses the issue of unbounded derivatives raised by the reviewer. Moreover, the stability constant C depends only on the problem coefficients and the fractional order γ, but not on the discretization parameters (M,k), which confirms the robustness of the method.

These findings are in line with fixed-point based convergence frameworks recently reported in the literature [25], while being specifically tailored here to pantograph-type problems with Mittag-Leffler wavelets. In addition, the present stability and convergence results are consistent with discrete maximum principle and error decomposition techniques developed in [4], which further validates the reliability of our approach in the broader context of fractional and singularly perturbed systems.

Declaration of competing interest

The authors declare that they have no known competing financial interests or personal relationships that could have appeared to influence the work reported in this paper.

Acknowledgements

The authors are very thankful to respected referees for their valuable comments.

References

[1] A.B. Albidah, N.E. Kanaan, A. Ebaid, H.K. Al-Jeaid, *Exact and numerical analysis of the pantograph delay differential equation via the homotopy perturbation method*, Math. **11** (2023) 944.

[2] H. Dehestani, Y. Ordokhani, M. Razzaghi, *A numerical technique for solving various kinds of fractional partial differential equations via Genocchi hybrid functions*, Rev. R. Acad. Cienc. Exactas Fís. Nat. Ser. A Mat. **113** (2019) 3297–3321.

[3] P. Das, S. Rana, *Theoretical prospects of fractional order weakly singular Volterra integro-differential equations and their approximations with convergence analysis*, Math. Methods Appl. Sci. **44** (2021) 9419–9440.

[4] P. Das, S. Natesan, *A uniformly convergent hybrid scheme for singularly perturbed system of reaction-diffusion Robin type boundary-value problems*, J. Appl. Math. Comput. **41** (2013) 447–471.

[5] P. Das, S. Rana, H. Ramos, *On the approximate solutions of a class of fractional order nonlinear Volterra integro-differential initial value problems and boundary value problems of first kind and their convergence analysis*, J. Comput. Appl. Math. **404** (2022) 113116.

[6] S. Dhama, *A reliable scheme for nonlinear delay differential equations of pantograph-type*, J. Comput. Sci. **75** (2024) 102206.

[7] A. Ghasempour, Y. Ordokhani, S. Sabermahani, *Fractional-order Mittag–Leffler functions for solving multi-dimensional fractional pantograph delay differential equations*, Iran. J. Sci. **47** (2023) 885–898.

[8] J. Hajishafieiha, S. Abbasbandy, T. Allahviranloo, *A new numerical approach for solving the fractional non-linear multi-pantograph delay differential equations*, Iran. J. Sci. **47** (2023) 825–835.

[9] N.A. Khan, M. Ali, A. Ara, M.I. Khan, S. Abdullaeva, M. Waqas, *Optimizing pantograph fractional differential equations: a Haar wavelet operational matrix method*, Partial Differ. Equ. Appl. Math. **11** (2024) 100774.

[10] M.A. Iqbal, M. Shakeel, S.T. Mohyud-Din, M. Rafiq, *Modified wavelets-based algorithm for nonlinear delay differential equations of fractional order*, Adv. Mech. Eng. **9(4)** (2017).

[11] M. Izadi, Ş. Yüzbaşı, K.J. Ansari, *Application of Vieta–Lucas series to solve a class of multi-pantograph delay differential equations with singularity*, Symmetry **13** (2021) 2370.

[12] H. Jafari, M. Mahmoudi, M.H. Noori Skandari, *A new numerical method to solve pantograph delay differential equations with convergence analysis*, Adv. Differ. Equ. **2021** (2021) 129.

[13] R.P. Meilanov, R.A. Magomedov, *Thermodynamics in fractional calculus*, J. Eng. Phys. Thermophys. **87** (2014) 1521–1531.

[14] S. Mashayekhi, M. Razzaghi, M. Wattanataweekul, *Analysis of multi-delay and piecewise constant delay systems by hybrid functions approximation*, Differ. Equ. Dyn. Syst. **24** (2016) 1–20.

[15] N. Negero, and G. Duressa, *An efficient numerical approach for singularly perturbed parabolic convection-diffusion problems with large time-lag*, J. Math. Model. **10(2)** (2022) 173-190.

[16] S. Nemati, P. Lima, S. Sedaghat, *An effective numerical method for solving fractional pantograph differential equations using modification of hat functions*, Appl. Numer. Math. **131** (2018) 174–189.

[17] Z. Odibat, V.S. Erturk, P. Kumar, V. Govindaraj, *Dynamics of generalized Caputo type delay fractional differential equations using a modified predictor-corrector scheme*, Phys. Scr. **96** (2021) 125213.

[18] Z. Odibat, V.S. Erturk, P. Kumar, A. Ben Makhlouf, V. Govindaraj, *An implementation of the generalized differential transform scheme for simulating impulsive fractional differential equations*, Math. Probl. Eng. 2022 (2022).

[19] I. Podlubny, *Fractional Differential Equations*, Academic Press, New York, 1999.

[20] I. Podlubny, Geometric and physical interpretation of fractional integration and fractional differentiation. arXiv preprint math/0110241. 2001

[21] K. Rabiei, Y. Ordokhani, *Solving fractional pantograph delay differential equations via fractional-order Boubaker polynomials*, Eng. Comput. **35** (2019) 1431–1441.

[22] P. Rahimkhani, Y. Ordokhani, E. Babolian, *A new operational matrix based on Bernoulli wavelets for solving fractional delay differential equations*, Numer. Algorithms **74** (2017) 223–245.

[23] P. Rahimkhani, Y. Ordokhani, *A computational method based on Legendre wavelets for solving distributed order fractional diffrential equations*, J. Math. Model. **9(3)** (2021) 501-516.

[24] S. Santra, J. Mohapatra, P. Das, D. Choudhuri, *Higher order approximations for fractional order integro-parabolic partial differential equations on an adaptive mesh with error analysis*, Comput. Math. Appl. **150** (2023) 87–101.

[25] D. Sarkar, S. Kumar, P. Das, H. Ramos, *Higher-order convergence analysis for interior and boundary layers in a semi-linear reaction-diffusion system networked by a k-star graph with non-smooth source terms*, Netw. Heterog. Media **19** (2024).

[26] M. Senol, M. Gencyigit, M.E. Koksal, S. Qureshi, *New analytical and numerical solutions to the (2+1)-dimensional conformable cpKP–BKP equation*, Opt. Quant. Electron. **56** (2024) 352.

[27] P. Vichitkunakorn, T.N. Vo, M. Razzaghi, *A numerical method for fractional pantograph differential equations based on Taylor wavelets*, Trans. Inst. Meas. Control **42** (2020) 1334–1344.

[28] B. Yuttanan, M. Razzaghi, T.N. Vo, *Legendre wavelet method for fractional delay differential equations*, Appl. Numer. Math. **168** (2021) 127–142.

[29] Ş. Yuzbaşı, N. Ismailov, *A Taylor operation method for solutions of generalized pantograph type delay differential equations*, Turk. J. Math. **42** (2018) 395–406.